SPE 38290

Linear Transient Flow Solution for Primary Oil Recovery with Infill and Conversion to Water Injection

Eric D. Zwahlen, Lawrence Berkeley National Laboratory, and Tad W. Patzek, SPE, University of California, Berkeley

This paper was prepared for presentation at the 1997 SPE Western Regional Meeting held in Long Beach, California, 25–27 June 1997.

Abstract

We present analytical solutions for primary production, producer infills and early response to waterflood in a low permeability, compressible, layered reservoir filled with oil, water and gas. The sample calculations are for the California Diatomites, but the equations apply to other tight rock systems. Primary oil recovery from rows of hydrofractured wells in a low permeability reservoir is described by linear transient flow of oil, water and gas with the concomitant pressure decline. During primary, it may be desirable to drill infill wells to accelerate oil production. At some later time, the infill wells may be converted into waterflood injectors for pressure support and incremental oil recovery. In this paper, we analyze the pressure response and fluid flow rates due to the original wells and infill wells drilled halfway between the original wells, and - finally - due to water injection at the infill wells. All of the formation and fluid properties are described by a single hydraulic diffusivity, α, assumed to be independent of time and production or injection. We solve the one-dimensional pressure diffusion equation analytically using pressure boundary conditions at the original and infill wells and use superposition to account for the water injection. We give solutions for the pressure in the formation and discuss how to calculate oil, water and gas rates and cumulatives as functions of time at both the original wells and infill wells. Finally, we present a computational example of oil production from a stack of seven diatomite layers with different properties and show the effects of infill wells and water injection on the total oil production. We show that results of this analytical solution and a compositional numerical simulation for primary production in the diatomite agree well. Our analysis can predict the onset of pressure depletion and quantify how long to produce from the infill wells before injecting water. It shows that producing from the infill well for a few years significantly increases the production from the field and can minimize the lost production at the infill well due to conversion to a waterflood injector. Our analysis also generates very reliable, well-by-well, field-wise forecasts of fluid production and water injection.

Introduction

The late and middle Miocene diatomaceous oil fields in the San Joaquin Valley, California, are located in Kern County, some forty miles west of Bakersfield. An estimated original-oil-in-place in the Monterey diatomaceous fields exceeds 10 billion barrels and is comparable to that in Prudoe Bay in Alaska.

Cyclic bedding of the diatomite[1] is a well documented phenomenon, attributed to alternating deposition of detritus beds, clay, and biogenic beds. The cycles span length-scales that range from a fraction of an inch to tens of feet, reflecting the duration of depositional phases from semi-annual to thousands of years. On a large scale, there are at least seven distinct oil producing layers with good lateral continuity within each layer, but little vertical continuity between adjacent layers. The diatomaceous rocks are very porous (25-65 percent), rich in oil (35-70 percent), and nearly impermeable (0.1-10 millidarcy). The high porosity and oil saturation, together with large thickness (up to 1000 feet) and area (up to a few square miles per field) translate into the gigantic oil-in-place estimates.

To compensate for the low reservoir permeability, all wells in the diatomite must be hydrofractured. A typical well has 3-8 fractures with an average fracture half-length of 150 feet. Wells are usually spaced along lines following the maximum in-situ stress every 330 feet (2-1/2 acre), 165 feet (1-1/4 acre) or even 82 feet (5/8 acre). Thousands of hydrofractures have been already induced and thousands more may be created as new recovery processes, such as waterflood[2-4] or steam drive[5-6] on 5/8 acre spacing, become commercially viable.

Primary oil production on 2-1/2 acre spacing, followed by infill to 1-1/4 acre and subsequent conversion to waterflood is of great interest to the producers of the diatomaceous oil

fields. **Fig. 1** shows a schematic of the production and infill process. We start from the mathematical formulation of the problem and present analytical solutions. We then present a computational example of a seven-layer diatomite reservoir. We also compare this analytical solution for primary production to a 1-D compositional reservoir simulation. Finally we match, well-by-well, the oil production and water injection in a waterflood project and perform rank order statistics.

Problem Statement

In a compressible, homogeneous porous medium, the pressure distribution follows a simple diffusion equation. With suitable boundary conditions and an initial condition, the pressure and fluid velocity in the medium can be calculated analytically. In this paper we present the governing equations and some graphical results for primary production, infill production, and finally water injection in the infill wells. See ref. 7 for a more complete derivation and listing of the solution equations.

We begin with a reservoir at some uniform initial pressure p_i at $t = 0$. First, we drill a series of wells with spacing $2L$ and wellbore flowing pressure p_{well} as shown in **Fig. 2**. All wells are hydrofractured, and all of the fractures are rectangular and have permeabilities that are much higher than the formation permeability. Therefore, we can assume that the uniform pressure p_{well} is imposed throughout the entire hydrofracture. Second, at some time t_{inf}, we drill infill wells halfway between the original wells and also produce these wells at p_{well}. Third, at time t_{inj}, we inject water into the infill wells at the downhole injection pressure p_{inject} and continue producing at the original wells. This final step is to quantify the effect of re-pressurization of the formation.

This statement of primary production, followed by infill and injection, is a simplification of what actually occurs in practice. Here we assume uniform and constant properties in each layer, constant pressures in the wells, and we neglect the effect production and injection may have on fluid and rock properties. We assume each of the layers in the reservoir is independent and solve the problem for each layer separately. These assumptions allow us to derive an analytical solution that can teach us the effect of each of the parameters on the production.

Original Primary Production. The one-dimensional pressure diffusion equation is

$$\frac{\partial p}{\partial t} = \alpha \frac{\partial^2 p}{\partial x^2}, \quad 0 \le x \le L, \quad t > 0 \qquad (1)$$

where

$$\alpha = \frac{\lambda_t}{\phi c_t} \qquad (2)$$

is the hydraulic diffusivity which accounts for the total compressibility of the formation, c_t, and the total fluid mobility, λ_t. All of the formation and fluid properties are combined into the single constant parameter α. For larger values of α, the pressure response will be faster. As mentioned, we assume α remains constant during production and injection.

From symmetry, we write the equations only for $0 \le x \le L$, while the original wells are at $x = \pm L$. The initial condition is uniform pressure everywhere in the layer,

$$p(x,0) = p_i, \quad 0 \le x \le L \qquad (3)$$

The boundary conditions for primary production are

$$\left.\begin{aligned} \frac{\partial p}{\partial x}(0,t) &= 0 \\ p(L,t) &= p_{well} \end{aligned}\right\}, \quad t < t_{inf} \qquad (4)$$

Before the infill time, the symmetry halfway between the original wells at $x = 0$ requires a no-flow boundary condition, which is specified by the gradient of the pressure being equal to zero. The pressure at the primary production well at $x = L$ is specified as the well flowing pressure.

This system of equations can be solved by separation of variables.[8] The zero gradient condition at $x = 0$ leads to a cosine expansion of the initial condition. The pressure before infill is

$$p(x,t) = p_{well} + 2(p_i - p_{well}) \sum_{n=0}^{\infty} (-1)^n \frac{\cos(\lambda_n x / L)}{\lambda_n} e^{-\lambda_n^2 \alpha t / L^2}, \qquad (5)$$
$$0 \le x \le L, \quad 0 < t < t_{inf}$$

where

$$\lambda_n = (2n+1)\frac{\pi}{2}, \quad n = 0, 1, 2, \ldots \qquad (6)$$

This cosine series clearly shows that the boundary conditions before the infill time are satisfied. The time dependence of the pressure is controlled by α divided by L^2.

We note that solving the problem by Laplace Transform leads easily to an error function solution better suited for early times

$$p(x,t) = p_{well} + (p_i - p_{well}) \times \left[1 - \sum_{n=0}^{\infty} (-1)^n \left\{ \operatorname{erfc} \frac{(2n+1) - x/L}{2\sqrt{\alpha t / L^2}} + \operatorname{erfc} \frac{(2n+1) + x/L}{2\sqrt{\alpha t / L^2}} \right\}\right] \qquad (7)$$
$$0 \le x \le L, \ t < t_{inf}$$

Primary After Infill. At the infill time, an infill well is drilled at $x = 0$, and the pressure is specified at both boundaries of the system. This set of boundary conditions leads to a sine series expansion of the original cosine series. We set $t = t_{inf}$ in (5) and use the result as the initial condition for a new set of side conditions to solve (1). The initial condition is

$$p(x,t_{inf}) = p_{well} + 2(p_i - p_{well})\sum_{n=0}^{\infty}(-1)^n \frac{\cos(\lambda_n x/L)}{\lambda_n} e^{-\lambda_n^2 \alpha t_{inf}/L^2}, \quad 0 \le x \le L \quad (8)$$

The boundary conditions are specified as constant pressure conditions by

$$\left.\begin{aligned} p(0,t) &= p_{well} \\ p(L,t) &= p_{well} \end{aligned}\right\}, \quad t \ge t_{inf} \quad \text{.....(9)}$$

Again by separation of variables, the solution to (1) is given by

$$p(x,t) = p_{well} + 4(p_i - p_{well})\sum_{m=1}^{\infty}\beta_m \sin(\beta_m x/L) e^{-\beta_m^2 \alpha (t-t_{inf})/L^2} \sum_{n=0}^{\infty}\frac{(-1)^n e^{-\lambda_n^2 \alpha t_{inf}/L^2}}{\lambda_n(\beta_m^2 - \lambda_n^2)}, \quad (10)$$

$$0 \le x \le L, \quad t > t_{inf}$$

where

$$\beta_m = m\pi, \qquad m = 1, 2, 3, \ldots \quad \text{.....(11)}$$

Oil Flow Rate Before Infill. The oil flow rate is proportional to the pressure gradient in the reservoir. The oil flow rate at the original primary wells $q_o^{(1)}$ is given by

$$q_o^{(1)} = -A\frac{kk_{ro}}{\mu_o}\left.\frac{\partial p}{\partial x}\right|_{x=L} \quad \text{.....(12)}$$

where A is *twice* the area of the production well hydrofractures, with the factor of 2 coming from symmetry (there are actually two production wells or, alternatively, two sides of a hydrofracture). The superscript (1) refers to the original wells. Differentiating the pressure solution in (5) and using the definition of the flow rate gives the flow rate before infill

$$q_o^{(1)} = 2A\frac{kk_{ro}}{\mu_o}\frac{(p_i - p_{well})}{L}\sum_{n=0}^{\infty} e^{-\lambda_n^2 \alpha t/L^2}, \quad 0 \le t \le t_{inf} \quad \text{.....(13)}$$

Differentiating (7) gives a form of the flow rate equation which is better suited for early times and clearly shows the square root of time dependence

$$q_o^{(1)} = A\frac{kk_{ro}}{\mu_o}\frac{(p_i - p_{well})}{\sqrt{\pi\alpha t}}\left\{1 + 2\sum_{n=1}^{\infty}(-1)^n e^{-\left(\frac{n}{\sqrt{\alpha t/L^2}}\right)^2}\right\}, \quad \text{.....(14)}$$

$$0 \le x \le L, \ t < t_{inf}$$

For early times, the summation is negligible because the exponential terms are approximately zero.

Oil Flow Rate After Infill. After the infill well is drilled, oil is produced from both the original primary well and the new infill well. After infill, the oil flow rate can be obtained by differentiating (10) and using (12) at $x = 0$ for the infill well and $x = L$ for the original well.

Cumulative Oil Production. We are interested in the total amount of oil that is produced from the original wells and the infill wells. The cumulative oil production up to some time t is given by

$$Q_o = \int_0^t q_o\, dt' = -A\frac{kk_{ro}}{\mu_o}\int_0^t \left.\frac{\partial p}{\partial x}\right|_{\substack{x=0 \\ or \\ x=L}} dt' \quad \text{.....(15)}$$

In the integration, we use (5) up until the infill time and (10) after the infill time. The pressure gradient from (5) is zero at $x = 0$ until the infill time so there is no contribution to the production at $x = 0$ until the infill well is drilled.

Water Injection at Infill Well. Finally, we investigate the effect of water injection at the infill well in order to re-pressurize the formation. We admit this approach is only approximate for water injection as it neglects the effect of incompressible Buckley-Leverett displacement of the oil by the injected water, as well as water imbibition. We assume the rock and fluid properties continue to be the same as originally present in the formation, and will use the same α. We then calculate the pressure in the system, the rate of injection and cumulative injection of water, and the rate and cumulative production of oil at the original well.

Because of the linearity of the equations, this water injection problem can be solved by superposition. We continue to calculate the pressure, flow rate, and cumulative production at the infill well using the equations previously discussed. The total pressure, injection, and production will be the sum of the previous infill problem and the following injection problem. The equations for the water injection calculation are

$$\frac{\partial p_{inj}}{\partial t} = \alpha\frac{\partial^2 p_{inj}}{\partial x^2}, \quad 0 \le x \le L, \quad t > t_{inj} \quad \text{.....(16)}$$

For *simplicity*, we use the same hydraulic diffusivity α in this injection problem as in the previous infill problem to describe the compressibility of the formation and the fluids. The initial condition is

$$p_{inj}(x,t_{inj}) = p_{well}, \quad 0 \le x \le L \quad \text{.....(17)}$$

This states that the initial pressure for this injection superposition calculation is the well flowing pressure.

The boundary conditions are constant pressure:

$$\left.\begin{aligned} p_{inj}(0,t) &= p_{inject} \\ p_{inj}(L,t) &= p_{well} \end{aligned}\right\}, \quad t > t_{inj} \quad \text{.....(18)}$$

The pressure at the infill well (now an injector) is prescribed as p_{inject} and the pressure at the original production well is prescribed as p_{well}.

We define a normalized pressure that scales the injection pressure to the original formation pressure

$$p^* = \frac{p_{inject} - p_{well}}{p_i - p_{well}} \quad \text{.....(19)}$$

The solution for the pressure in the formation due only to water injection is a sine series

$$p_{inj}(x,t) = p_{well} + p^*(p_i - p_{well})\left\{1 - \frac{x}{L} - 2\sum_{m=1}^{\infty}\frac{\sin(\beta_m x/L)}{\beta_m} e^{-\beta_m^2 \alpha (t-t_{inj})/L^2}\right\}, \quad (20)$$
$$0 \le x \le L, \qquad t > t_{inj}$$

We differentiate this pressure solution with respect to x to get the water flow rate in the absence of oil pressure as in (12). The flow rate at x = 0 is the water injection rate, and the flow rate at x = L is production at the original well. We can then integrate this injection rate solution over time using (15) to get the cumulative water injection, again in the absence of the flowing oil.

Total Pressure, Flow Rates, and Cumulative Production by Superposition. We are actually interested in the total (or net) pressure, flow rates and cumulative production including the original infill solution and this water injection solution. We now present the superposition equations necessary to calculate the net pressure, flow rates, and cumulative production after water injection begins. The linearity of the equations allows us to add the results of the infill problem to the results of the injection problem to get the total. The following equations are valid for $t > t_{inf}$. The superscripts (1) and (2) refer the original and infill wells, respectively.

The total pressure in the formation is sum of the pressure calculated by the original solution for p and the solution for p_{inj}

$$p^{net} = p + p_{inj} - p_{well}, \qquad t > t_{inj} \quad \text{.....(21)}$$

The net oil production rate at the original well $q_o^{(1),net}$ is the sum of the oil flow rates from the infill problem and the injection problem

$$q_o^{(1),net} = q_o^{(1)} + q_{o,inj}^{(1)}, \qquad t > t_{inj} \quad \text{.....(22)}$$

Similarly, the net cumulative oil production at the original well is

$$Q_o^{(1),net} = Q_o^{(1)} + Q_{o,inj}^{(1)}, \qquad t > t_{inj} \quad \text{.....(23)}$$

The net rate of water injection is given by the water injection rate from the injection problem minus the oil production rate calculated from the original infill problem,

$$q_{w,inj}^{(2),net} = q_{w,inj}^{(2)} - q_o^{(2)}, \qquad t > t_{inj} \quad \text{.....(24)}$$

The net cumulative production at the infill well is slightly more complicated. After water injection begins at the infill well, there is no more oil production from this well. We let $Q_{o,inj}^{(2)}$ be the cumulative oil production at the infill well up until the time at which water injection begins. Then the net cumulative water injection is given by

$$Q_w^{(2),net} = Q_{w,inj}^{(2)} - \left(Q_o^{(2)} - Q_{o,inj}^{(2)}\right), \qquad t > t_{inj} \quad \text{.....(25)}$$

Computational Example – Single Well

As an example, we model an average well in Section 33 of the South Belridge diatomite field. This region can be divided into seven separate layers (diatomite cycles), each with its own material and fluid properties. For each layer, we assume that the initial producer spacing is 330 feet (2-1/2 acre), and the tip-to-tip length of the hydrofracture is also 330 feet. The important properties of each layer are summarized in **Figs. 3-5**. These data are averages of well logs taken at 1-foot intervals through the reservoir column.

Fig. 3 shows the amount of oil in each layer calculated as $S_o\phi h$, which when multiplied by the pattern area gives the OOIP. The depths and thicknesses of each layer are shown on the vertical axis. Layer G is the thickest and has a high oil saturation giving it a large volume of oil. Layer K is very thin, so it has little oil to produce. The remaining layers are between those extremes.

Fig. 4 shows the formation absolute permeability for each layer, again as a function of depth. The permeability starts at 0.15 md in the upper layers, is slightly higher towards the bottom, and jumps to 0.85 md in layer M.

More important than the absolute permeability is the absolute permeability times the oil relative permeability, kk_{ro} shown in Fig. 5. We use the Stone II model with reasonable coefficients and exponents to calculate the oil relative permeability. Large values of kk_{ro} are desirable so layers G and K are good, while layer I is obviously poor.

To get a quantitative estimate of the productivity of a layer, we must calculate its hydraulic diffusivity, α. We use general correlations[9-11] for the viscosity, mobility, and compressibility and give the results in **Fig. 6**.

Layer K has the highest α and will react the fastest and produce well. However, it is a thin layer with little oil in place so the total volume will be small. Layers G, J, L, and M have intermediate values of α and good amounts of oil, so they will be good producers. Layers H and I have the lowest values of α and will produce poorly and show little effect of infill and water injection.

We assume that the layer pressure corresponds to the oil bubble-point pressure for a particular layer. The bubble point pressure as a function of depth is given by

$$p_{bp} = 29.7 + 0.438 \times \text{depth(ft)}, \quad \text{psia} \quad \text{.....(26)}$$

The layer temperature is calculated from the average thermal gradient for the diatomite which is given as

$$T = 72.0 + 0.024 \times \text{depth(ft)}, \quad ^\circ\text{F} \quad \text{.....(27)}$$

For the calculations we impose a back-pressure of 50 psia on the producers. The original wells produce for 10 years (3650 days) after which an infill well is drilled between the original wells. After one year of production from the infill well, at 11 years (4015 days), water is injected at p_{inject} into the infill well, where

$$p_{inject} = 0.7 \times \text{depth(ft)}, \quad \text{psia} \quad \text{.....(28)}$$

These parameter values are used to calculate the pressure, oil flow rate at the wells, and cumulative oil production from each layer as a function of time for 50 years (18250 days = 135 day$^{1/2}$).

Fig. 7 shows the cumulative primary production in thousands of barrels in each layer and the total for 50 years without infill or injection. The slope of the total primary production is approximately 3000 barrel/day$^{1/2}$, which is representative of a very good well in the diatomite. A poorer well might not have the entire hydrofracture area open and the production would be less.

Layer G, which has the most oil in place and high α, produces the most oil. The next two layers, H and I, have low oil saturations and low α values, and are poor producers. The deeper layers have high α values and are good producers. Layer K has a low cumulative production because it has little oil in place.

Fig. 8 shows the percent oil recovery of all of the layers and the total for 50 years. The total is recovery is about 10 percent with the deeper layers J through M better, and the top layers G through I worse.

Fig. 9 shows the pressure profiles for infill at 10 years and water injection at 11 years for layers G, I, K, and M. These layers show representative values of α with layer I being the lowest and layer K the largest. Large values of α give faster pressure response. In these figures, the position labeled 0 feet is the position of the infill well, and the position at 165 feet is the original well. The pressure at the original well is constant at 50 psia.

In Fig. 9a, the initial pressure in layer G is 350 psia and the pressure at the "original" well is maintained at 50 psia. The pressure profile at $x = 0$ is horizontal until 10 years indicating the no-flow (or symmetry) boundary condition. At 10 years when the infill well is drilled, the pressure at $x = 0$ has not decreased significantly. The 11th year profile is just before injection at 513 psia begins at the infill well. Finally, the pressure distribution becomes a linear, steady-state profile with injection.

Layer I, shown in Fig. 9b, reacts much more slowly than the other layers. The initial pressure is 480 psia. By 10 years when the infill well is drilled, the pressure wave is only about a quarter of the way in from the original well. Even at 50 years, the steady-state is not yet reached. The infill and injection does not significantly affect the original well.

Layer K, shown in Fig. 9c, has the highest α, and the pressure wave reaches the infill well position at 5 years. By 10 years the pressure has dropped enough so that oil production at the original well is also falling. After injection begins, the steady-state is nearly reached in 15 to 20 years.

Layer M, shown in Fig. 9d, appears very similar to layer G. Even though layers G and M have different properties, their α values are similar which results in similar pressure response times.

Fig. 10 shows the percent oil recovery or water injection for infill at 10 years and water injection at 11 years for each layer in the formation calculated as the volume produced or injected divided by the original oil in place times 100 percent. The final total increase in recovery due to injection is about 3 percent. The scale of each figure, except layer K, is the same so that the layers can be easily compared.

Each of the plots has five separate curves. The top curve, shown as a bold solid line, is the percent oil recovery from the original well, including the effect of the infill well and water injection. The upward trend at late times is due to the extra oil produced by water injection. The normal solid line is the percent oil recovery at the original well with infill but without injection at the infill well. In most of the layers, the difference between recovery with and without injection is about 3 percent. In layer K the effect is rapid and large, because of the high α. However, we stress that much of the increased recovery in this layer at late times may be just the injected water recirculated through the producer. Layers H and I show almost no effect of the water injection because of low oil saturation and low α. This calculation shows that in the absence of Buckley-Leverett banking of oil, the incremental oil recovery from pressure support by water injection will be small. Hence in layers with a low oil saturation or unfavorable mobility ratio, one cannot expect a big waterflood response.

The first dotted curves show the percent oil recovery at the infill well where production starts from zero at the infill time. The "Infill (no injection)" curves show the production if there were no injection, and the "Infill (with injection)" curves show the production with injection. These latter recovery curves (including water injection) become flat after water injection begins because no more oil is produced at the infill well. For most of the layers, a significant amount of oil production from the infill well is lost because of injection. However, injection may be necessary to preserve the integrity of the formation and decrease well failure. Thus, producing from the infill well for two to five years before injection begins instead of just one may be better.

The water injection curve is the volume of water injected divided by the original oil in place in the layer times 100 percent to keep the units consistent. Even though the injection begins at 11 years, the effect at the original wells is not seen until almost 20 years. Layer K shows the effect sooner, but layers H and I show almost no effect of injection even at 50 years. The rate of water injection becomes constant at late times so the percent water injection rises linearly with time for late times. However, it appears to bend upward when plotted here versus the square root of time.

To further explain the figures, we specifically consider layer G. We see from Fig. 7 that the total volume of oil produced in 50 years is approximately 100 MSTBO with no infill or injection, which is about 8 percent recovery. With infill and injection, the original well produces just under 9 percent or 110 MSTBO, and the infill well produces an additional 15 MSTBO in the one year of production. The 15

MSTBO could be increased to about 30 MSTBO, if water injection began at 13 years instead of 11.

Comparison with THERM® Simulator

We now compare the results of this analytical solution with a 1-D simulation done with a reservoir simulator, THERM. The numerical simulation is of primary production on 2-1/2 acres. As shown in **Figs. 11 and 12**, the two analyses give nearly the same results. The data for these simulations are for a deep layer, e.g. layer M, but having a moderate permeability and high oil saturation. The depth in the analytical solution was chosen to match the initial pressure in the numerical simulation. The well flowing pressure is fixed at 100 psia in both cases. The only parameters that are different in the two calculations are kk_{ro} and μ_o, where kk_{ro} = 0.7 md and 0.8 md and μ_o = 4.5 cp and 5-6 cp in the analytical and numerical simulations, respectively.

Fig. 11 compares the percent oil recovery. The numerical simulation is carried to 36 years and the analytical solution to 50 years. Until the very end of the simulation the results are similar. The numerical simulation predicts a lower ultimate recovery, probably because depletion changes the properties of the system. Thus α is not actually constant for the entire production time. However, the differences are not significant until after 30 years.

Fig. 12 compares the average pressure in the layer. The average pressure predicted by the analytical solution falls slightly slower than that predicted by THERM. This is also evidenced by the slightly higher production shown in Fig. 11. Also, near the end of the simulation, the pressure flattens out more quickly, and the production slows down.

We see that our simple model can accurately predict the recovery and pressures for primary production. The PVT properties of the general correlations and relative permeabilities agree well with those predicted by THERM.

Computational Example – Multiple Wells

As demonstrated above, our analytical model can be used to capture the detailed, layer-by-layer behavior of a single "typical" producer in the diatomite. On the other hand, Fig. 8 shows that while some reservoir layers suffer from pressure interference, the total cumulative production from this well is a remarkably straight line when plotted versus the square root of time for up to 50 years. A downward deviation from this line foreshadows pressure depletion, and an upward deviation is a sign of reservoir re-pressuring by water injection and, perhaps, of Buckley-Leverett displacement of the oil by the injected water. The latter mechanism is not modeled here.

Hence, Eq. (14) can be used to match and then forecast the oil, water and gas production, as well as water injection, for an entire field project. Here, we will simplify this equation, so that only the square-root-of-time behavior of individual wells is retained. In other words, we neglect the late-time well interference.

As an illustration, we use the Crutcher-Tufts waterflood project in Sections 1 and 12 of the Dow-Chanslor Fee in the Middle Belridge Diatomite, Kern County, CA **(Fig. 13).** Because of the page limit, we focus here on Section 1 alone, but we perform rank order statistics on all 121 producers and 37 water injectors in both sections.

The input data are ASCII-format queries from a Production Analyst® database for Dow-Chanslor. The monthly well records for each producer include the current calendar time, the number of days on production in a given month, and the monthly produced oil, gas and water. For injectors, the monthly records consist of the calendar time, the number of days on injection (if available), the injected water, and the average wellhead pressure (WHP). These data are processed by our custom software package which performs the production and injection forecasts.

Our software can calculate the oil, gas and water production rates for a typical well in a project. This is done by calculating the elapsed times on production (the elapsed calendar time minus the cumulative down time) for all producers which exist at a given calendar time. In other words, at a fixed calendar time, each well has its own cumulative time on production and the corresponding cumulative oil, gas and water production. The number of active wells varies with time. For example, at short elapsed times on production all wells are counted, and at the long times only the oldest wells enter the calculation. The result of this time shifting and averaging is shown in **Fig. 14**. In this particular case, the average slope of a producer "prototype" in Section 1 is 900 BO/$\sqrt{\text{Days on production}}$. As shown below, this procedure yields an average well with oil slope close to the mean of the underlying lognormal distribution of all oil slopes in a project. Thus the calculated average oil slope can be used to calculate the average oil rate versus time, **Fig. 15**. Both Figs. 14 and 15 show a short, 100 day, "startup period," which is excluded from the slope calculations. During this time period, wells are free-flowing and often must be cleaned up because of back-production of the hydrofracture proppant.

Our software can also fit, in the least-square sense, the oil, gas and water slopes for each producer in a project. This automatic procedure skips the initial start-up period and can be biased by the user against a late-time waterflood response or pressure depletion. The resulting sample of all possible oil slopes in a project can then be analyzed using the standard statistical methods. It is well known that any conclusions about sample properties, e.g., the mean slope, standard deviation, etc., are predicated on the *randomness* of the sample. Therefore, we must check if our sample is reasonably random. One way of checking this is to perform *order statistics*.[12] First, we sort the natural logarithms of oil slopes in order of increasing magnitude. These sorted values are called order statistics. Second, we transform these data to zero mean and unit standard deviation. Third, we calculate the cumulative area underneath the standard normal distribution that would be associated with each consecutive data point *if* it belonged to this distribution. Fourth, by iterating on the upper limit of the

standard normal distribution, we calculate the value of *normal variable* or deviate that corresponds to the cumulative area assigned to each sample point. Fifth, we plot the ordered sample values versus the calculated normal deviate, **Fig, 16**. If the sample comes from a single normal distribution, then this plot results in a straight line with the slope equal to the mean and the intercept equal to the standard deviation of the distribution. Thus a plot of **order statistics is useful in drawing inferences from a sample about the nature of the parent population**. If a sample consists of portions of distinctly different populations, then a detectable break ("kink") in the slope of the line results. Therefore, order statistics is also useful in judging the homogeneity of the sample (whether it belongs to the same parent population).

Fig. 16 shows that the productivities of all oil wells at Dow-Chanslor, expressed through their oil slopes, belong to a single lognormal population. This is plausible, because all producer hydrofractures are under compression and similar draw-downs. Hence the oil rate depends only on the product of active hydrofracture area and the oil mobility, modified by the total hydraulic diffusivity. This product ought to be distributed lognormally. The underlying population is depicted in **Fig. 17**. Its most probable value (mode) is 420, the middle sample value (median) is 717, and the equal-area value (mean) is 937 BO/Sqrt(D). The mean oil slope from the lognormal distribution is about the same as the average time-shifted slope in Fig. 14. It also follows that 99.7% of all existing or future producers at Dow-Chanslor should have slopes lower than 3300 BO/Sqrt(D), unless better and bigger hydrofractures are available.

An identical analysis may be performed for the injection wells. The time-shifted cumulative water injection versus the square root of time on injection is shown in **Fig. 18**. An average water slope is 34,500 BW/Sqrt(D). Note that the plot of cumulative water is not a straight line (cf. Fig. 14). The reason for this is shown in **Fig. 19,** as the history of average injector WHP's. The injection pressures are continually increased with time, thus accelerating the water injection relative to Eq. 14. Also, the injector fractures are under tension, have been designed differently over time, and undergo extensions. A more complex analysis, such as in ref. 2, should be used. Nevertheless, with an exception of the initial rate overshoot, the square-root-of-time model of water injection works reasonably well.

The rank order statistics of water injection slopes, **Fig. 20**, reveal at least two, and perhaps four, underlying populations. The old injectors, to the left of the mean, form one or two populations, and the new ones, to the right of the mean, also form one or two populations. However, the numbers of data points representing each sub-population are small. Thus, on average, all the water injectors at Dow-Chanslor can be thrown into one lognormal population, shown in **Fig. 21**. The population mode is 18,600, its median is 28,700 and the mean is 32,300 BW/Sqrt(D). This population is much wider than that shown in Fig. 17; all Dow-Chanslor injectors should have slopes less than 97,000 BW/Sqrt(D). This large population width reflects the different hydrofracture designs and the injector operation at different fractions of the overburden stress. A more detailed statistical analysis of injector behavior requires a larger data set and a linear superposition[2] approach. Such an analysis can be performed for larger projects, e.g., in the South Belridge Diatomite.

The ratio of the mean injector and producer slope is 35 BW/BO. Hence, from Eq. (14) it follows that

$$\frac{A_I}{A_P}\frac{k_I}{k_P}\frac{k_{rw}}{k_{ro}}\frac{\mu_o}{\mu_w}\sqrt{\frac{\alpha_P}{\alpha_I}}\frac{0.6}{1-116/h)} \approx 35 \quad \text{.....(29)}$$

This ratio cannot be explained by the relative permeabilities alone. The layer-thickness weighted relative permeability to oil in the single well example is about 0.2. One should expect the end-point water relative permeability to be no more than 0.2. The average ratio of the oil and water viscosity is about 6-10 and the square root of the respective hydraulic diffusivities is close to 1. Therefore,

$$\frac{A_I}{A_P}\frac{k_I}{k_P} \approx 6-10, \quad \text{.....(30)}$$

i.e., a combination of a larger active hydrofracture area and formation fracturing away from the injection hydrofracture may be responsible for such large slope ratios. Another possibility is that the producer hydrofractures plug with fines and precipitates.

Finally, our software can forecast the oil, gas and water production, and water injection, for an entire project or field. Two examples for Section 1 are shown in **Figs. 22 and 23**. Note how well our simple, one-parameter model captures the overall oil production. This model can be run into the future, resulting in a very reliable forecast of primary production. An upward deviation from the forecast is the waterflood response and a downward one is the formation damage and pressure interference.

In summary, we have demonstrated that an entire primary/waterflood project in the diatomite, or another low permeability rock, can be analyzed with our simple model. Also, production and injection forecasts, including future infills and conversions can be performed quite easily. Finally, as a byproduct of fitting the oil, gas and water slopes, an interesting insight into the reservoir productivity can be obtained. Water injectivity, one the other hand, is more difficult to analyze, but it also provides hints of the hydrofracture sizes and formation fracturing.

Conclusions

1. We have developed a complete analytical model of transient, linear, single phase flow in a low permeability, layered, and compressible reservoir and have presented results for primary fluid recovery from the original well spacing, followed by an infill program and conversion of the infill wells

to water injectors.

2. Our analysis is simplified and has many limiting assumptions. It is not meant to be a replacement for reservoir simulations but, being an analytical solution, it separates the effects of the various parameters on the solution. However, the calculations presented here for the South Belridge Diatomite should give reasonable estimates of the diatomite layer productivities. This simple solution agrees well with a THERM® reservoir simulation.

3. This analysis can give an estimate of when to drill an infill well and how long to produce from the infill well before converting it to an injector. Our analysis predicts that about 10% of OOIP can be recovered on 2-1/2 acre primary in a good portion of the south Belridge Diatomite. The infill to 1-1/4 acres, followed by a conversion of the infill well to a water injector, increases the ultimate recovery by another 3% of OOIP. Hence, in the absence of a strong Buckley-Leverett banking of the oil and/or strong capillary imbibition, the effect of pressure support by water injection on the incremental oil recovery is weak. In lower quality reservoirs (layers or fields) the effect of waterflood may be small.

4. Another important result is the quantification of reservoir heterogeneity. This analysis helps identify the good layers and those layers with fast pressure responses. The current analysis gives a good estimate for the pressure, production rate, and cumulative production from original wells, with infill producers drilled at some later time and then converted to water injectors. This model can predict the onset of pressure depletion and quantify the duration of production from the infill wells before injecting water. We have shown that producing from the infill well for a few years significantly increases the production from the field and can minimize the lost production at the infill well due to conversion to a waterflood injector.

5. We have demonstrated that the simplified Eq. (14) alone can match, well-by-well, the fluid production and injection for an entire primary/waterflood project in the diatomite (or another low permeability rock). The same simplified model can then be used to provide reliable primary production and water injection forecasts, including future infills and conversions. A positive deviation from the primary forecast is a sign of waterflood response and a negative one suggests pressure depletion and/or producer plugging.

6. As a byproduct of fitting the slopes of cumulative oil, gas and water production versus the square root of time, an interesting insight can be obtained into the reservoir productivity and the effective areas of producer hydrofractures. Water injectivity, one the other hand, is more difficult to analyze, but it also provides hints of the hydrofracture sizes and formation fracturing.

7. Finally, the current analysis can easily be incorporated into an economic model of an entire project or field.

Acknowledgments

This work was supported by two members of the U.C. Oil® Consortium, Chevron Petroleum Technology Company, and CalResources, LLC. Partial support was also provided by the Assistant Secretary for Fossil Energy, Office of Gas and Petroleum Technology, under contract No. DE-ACO3-76FS00098 to the Lawrence Berkeley National Laboratory of the University of California.

Nomenclature

A = twice the area of the production hydrofracture, ft^2
k_{ro} = relative permeability for oil
L = half-spacing of original wells, ft
m = summation index
n = summation index
p = pressure in analytical solution, psia
p_{bp} = bubble point pressure, psia
p_i = initial formation pressure, psia
p_{inj} = pressure in injection superposition equations, psia
p_{inject} = water injection pressure, psia
p_{net} = net (total) pressure with infill and injection, psia
p_{well} = well flowing pressure, psia
Q = cumulative amount, MB
q = flow rate, MBPD
T = temperature in the formation, °F
t = time after original production begins, days
t_{inf} = time when infill well begins production, days
t_{inj} = time when water injection begins, days
x = distance from centerline between original wells, ft
α = total fluid mobility, ft^2/day
β_m = eigenvalue
λ = mobility, md/cp
λ_n = eigenvalue
ϕ = porosity
μ = viscosity, cp

Subscripts

f = formation
g = gas
I = injector
inf = infill
inj = injection
o = oil
P = producer
t = total
w = water

Superscripts

(1) = original well
(2) = infill well
net = total including infill and injection

References

1. Schwartz, D. E.: "Characterizing the Lithology, Petrophysical Properties, and Depositional Setting of the Belridge Diatomite, South Belridge Field, Kern County, California," Studies of the

Geology of the San Joaquin Basin, S. A. Graham and H. C. Olson (eds.), The Pacific Section Society of Economic Paleontologists and Mineralogists, Los Angeles, CA (1988) 281-301.

2. Patzek, T. W.: "Surveillance of South Belridge Diatomite," paper SPE 24040 presented at the 1992 Soc. Pet. Eng. Western Regional Meeting, Bakersfield, Ca., Mar. 30 - Apr. 1.
3. Nikravesh, M., A. R. Kovscek, and T. W. Patzek: "Prediction of Formation Damage During Fluid Injection in to Fractured Low Permeability Reservoirs Via Neural Network," The SPE Formation Damage Symposium, Lafayette, La., February 14-15, 1995.
4. Nikravesh, M., A. R. Kovscek, A. S. Murer, and T. W. Patzek: "Neural Networks for Field-Wise Waterflood Management in Low Permeability, Fractured Oil Reservoirs," paper 35721 presented at the 66th Soc. Pet. Eng. Western Regional Meeting, Anchorage, Alaska, May 22-24, 1996.
5. Kovscek, A. R., R. M. Johnston, and T. W. Patzek: "Interpretation of Hydrofracture Geometry Using Temperature Transients I: Model Formulation and Verification," In Situ 9, (September 1996).
6. Kovscek, A. R., R. M. Johnston, and T. W. Patzek: "Interpretation of Hydrofracture Geometry Using Temperature Transients II: Asymmetric Hydrofractures," In Situ 9, (September 1996).
7. Zwahlen, E. D., and T. W. Patzek: "Linear Transient Flow Solution for Primary Oil Recovery with Infill and Conversion to Water Injection," to be published in In Situ.
8. Carslaw, H. S., and J. C. Jeager: Conduction of Heat in Solids, 2nd Ed., Clarendon Press, Oxford (1959).
9. Ahmed, T.: Hydrocarbon Phase Behavior, Contributions in Petroleum Geology and Engineering 7, Gulf Publishing Company, Houston, (1989) 424.
10. Standing, M. B.: A Pressure-Volume-Temperature Correlation for Mixtures of California Oils and Gases, SPE Drilling and Practice (1947) 275.
11. Beggs, H. D., and J. R. Robinson: "Estimating the Viscosity of Crude Oil Systems," Journal of Petroleum Technology 27 (1975) 1140-1141.
12. Mandel, J. "The Statistical Analysis of Experimental Data," Denver 1984.

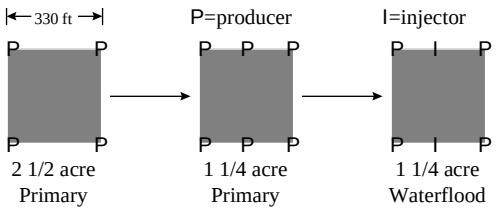

Fig. 1—Schematic of 2 1/2 acre primary followed by infill to 1 1/4 acres followed by conversion to water injection.

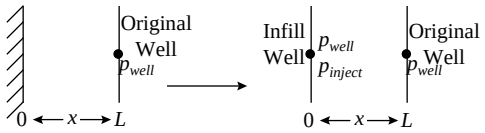

Fig. 2—Schematic for mathematical problem describing primary production followed by infill. Note the symmetry in the primary production at $x = 0$ leads to a no flow boundary. The wells are prescribed pressure boundaries.

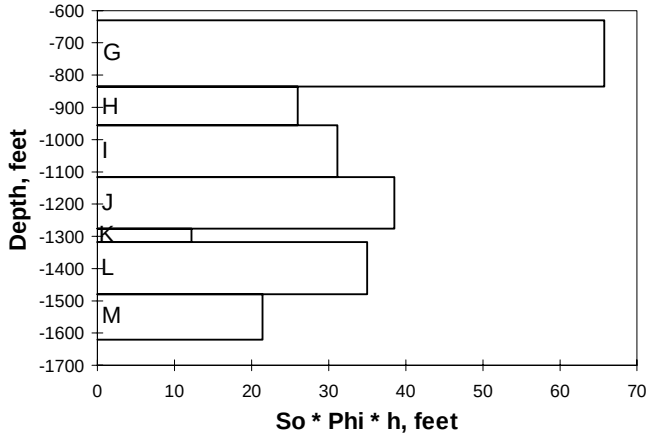

Fig. 3—Amount of oil per unit area of reservoir in each layer.

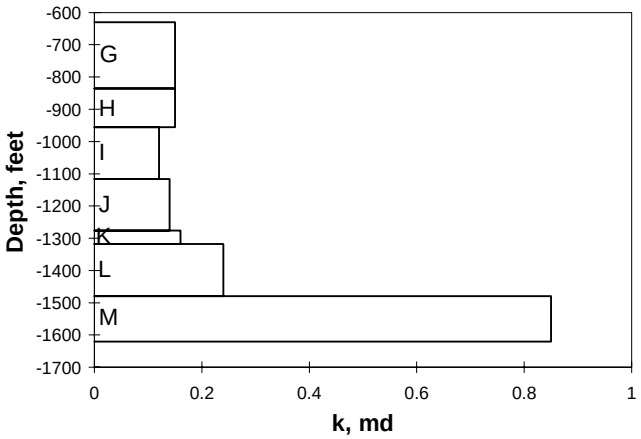

Fig. 4—Average diatomite layer permeability in millidarcies as a function of depth.

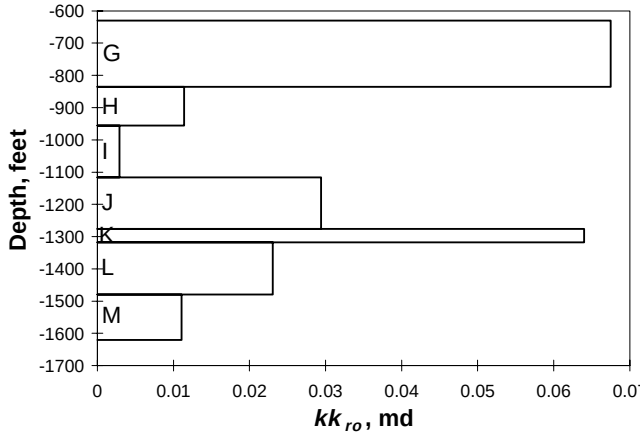

Fig. 5—Actual oil permeability in millidarcies for the diatomite layers.

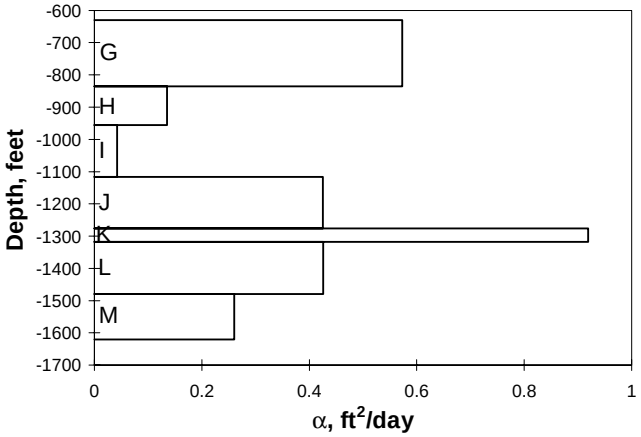

Fig. 6—Calculated α in ft^2/day for the diatomite layers.

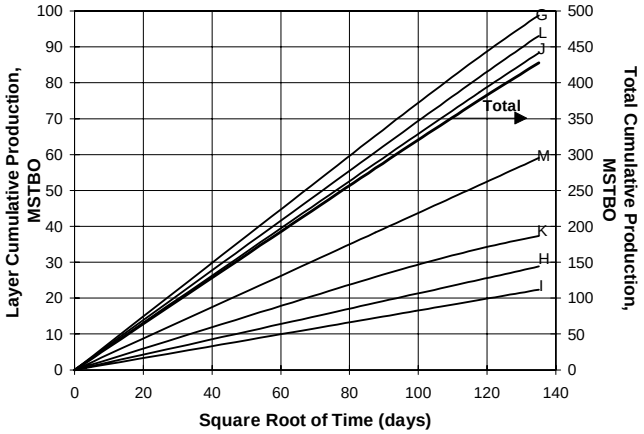

Fig. 7—Cumulative oil production in each layer. No infill or injection.

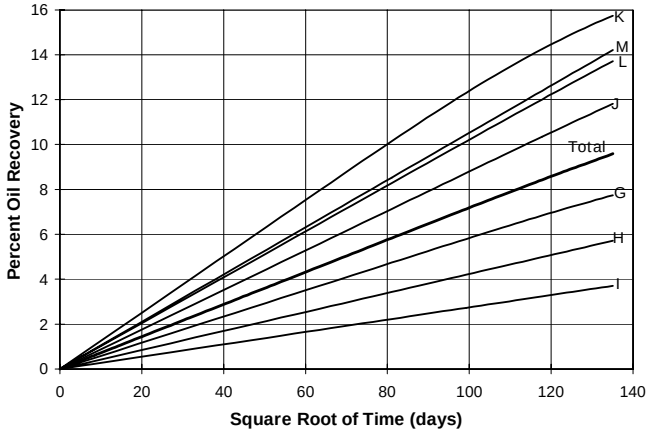

Fig. 8—Percent oil recovery in each layer. No infill or injection.

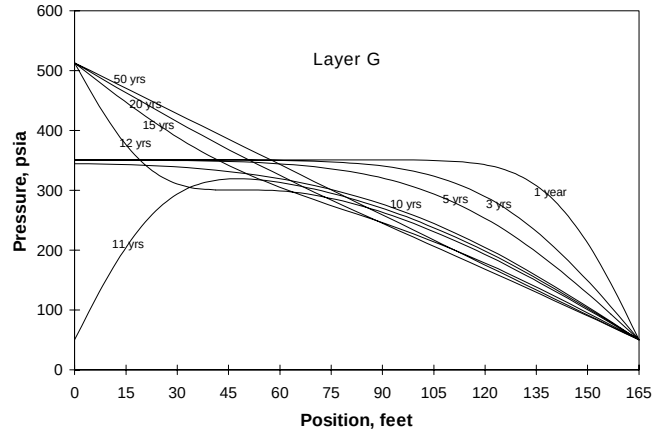

Fig. 9a—Pressure in layer G, psia, versus the position from infill well, feet. Infill at 10 years and injection at 11 years.

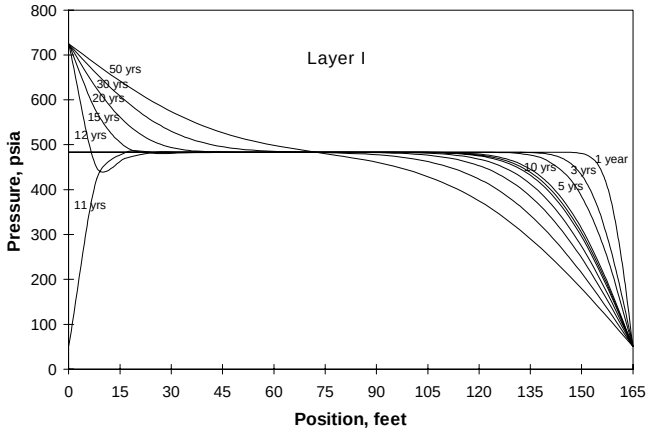

Fig. 9b—Pressure in layer I, psia, versus the position from infill well, feet. Infill at 10 years and injection at 11 years.

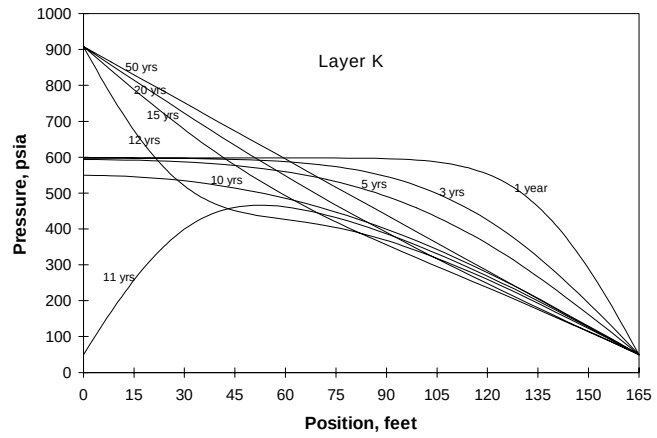

Fig. 9c—Pressure in layer K, psia, versus the position from infill well, feet. Infill at 10 years and injection at 11 years.

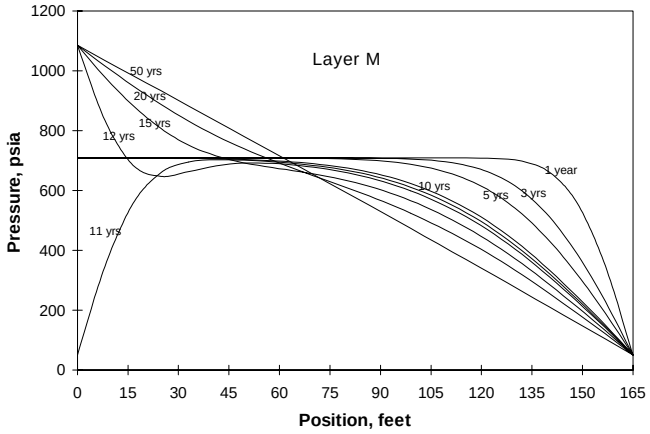

Fig. 9d—Pressure in layer M, psia, versus the position from infill well, feet. Infill at 10 years and injection at 11 years.

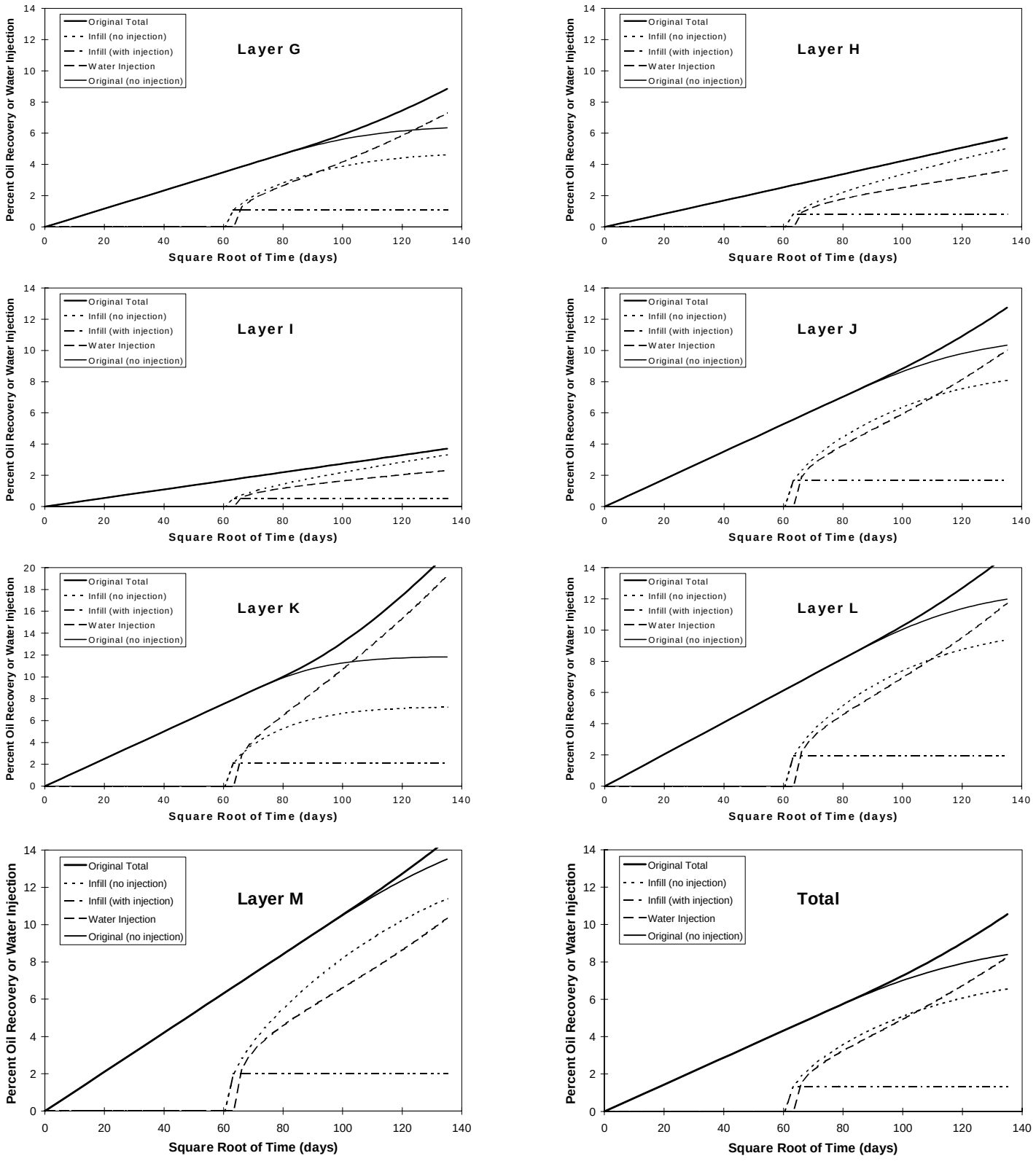

Fig. 10—Percent oil recovery or water injection versus the square root of time, days$^{1/2}$, calculated as the amount produced or injected divided by the original-oil-in-place times 100 percent. Infill at 10 years and injection at 11 years.

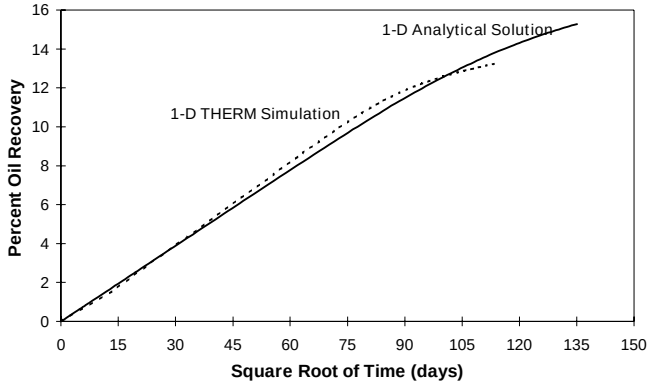

Fig. 11—Comparison of THERM simulation and analytical solution. Percent oil recovery on primary for 50 years.

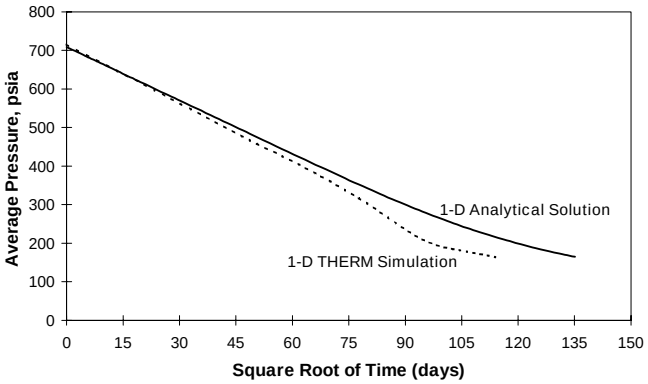

Fig. 12—Comparison of THERM simulation and analytical solution. Average layer pressure on primary for 50 years.

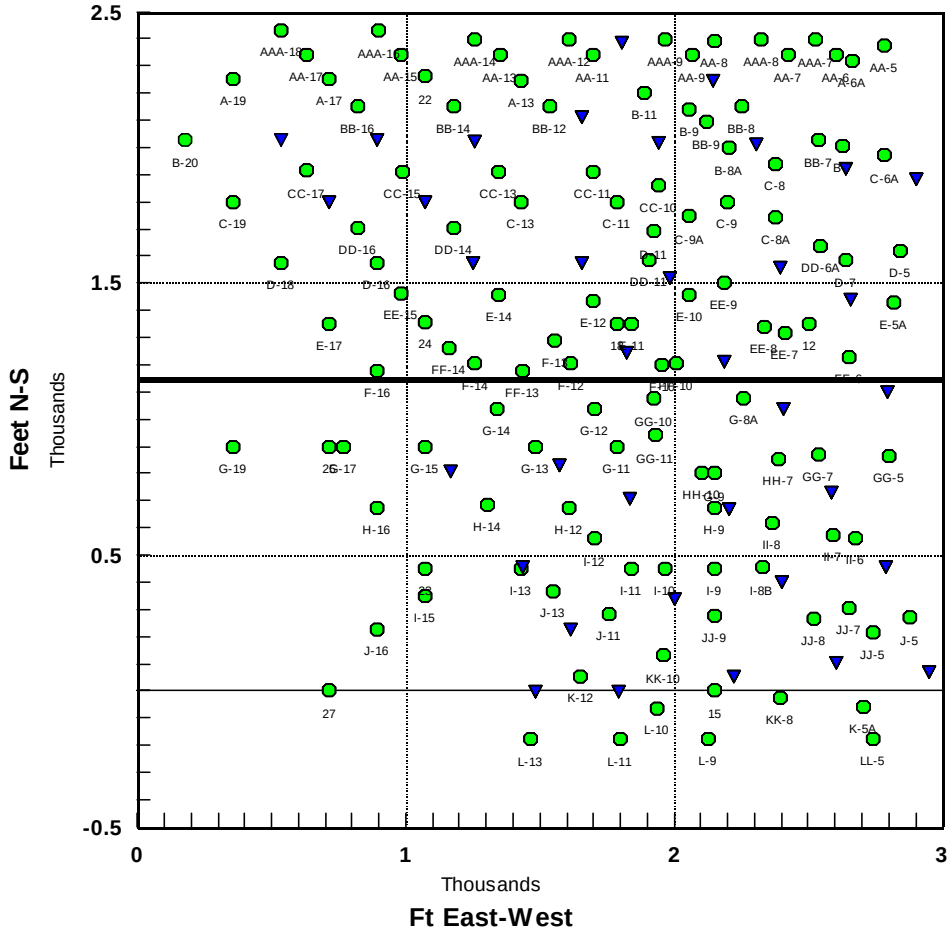

Fig. 13—The Crutcher-Tufts waterflood project in Sections 1 (the upper half) and 12 of the Dow-Chanslor Fee, Middle Belridge Diatomite, Kern County, CA. The triangles are water injectors.

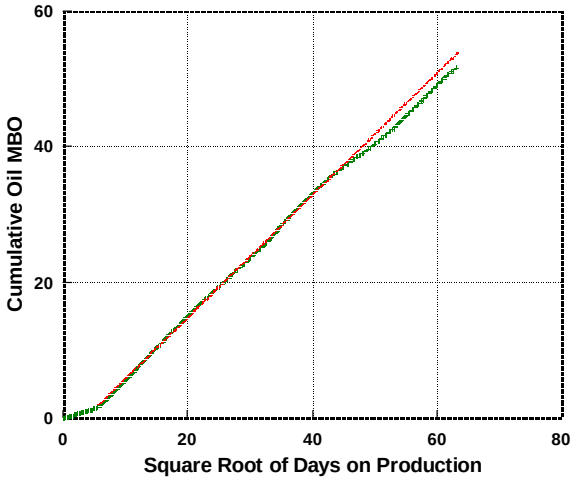

Fig. 14—Cumulative oil production from an average, time-shifted Crutcher-Tufts Section 1 well versus the square root of time. The average oil slope for 77 producers is 900 BO per square root of days on production. Note that only the oldest wells underperform the single trend above.

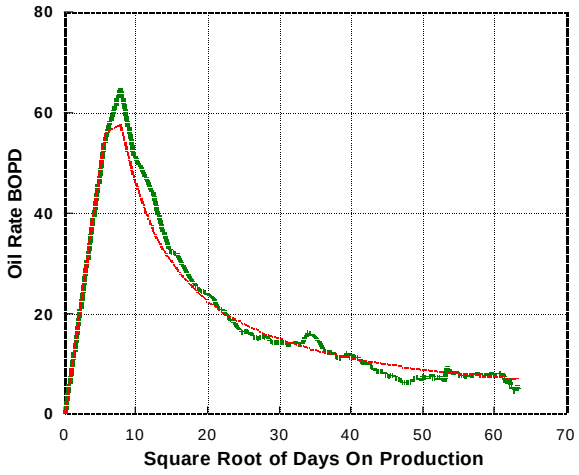

Fig. 15—Oil production rate from an average, time-shifted Crutcher-Tufts Section 1 well versus the square root of time. This is the oil rate expected from an average well in Section 1. Note a 100-day "startup-period."

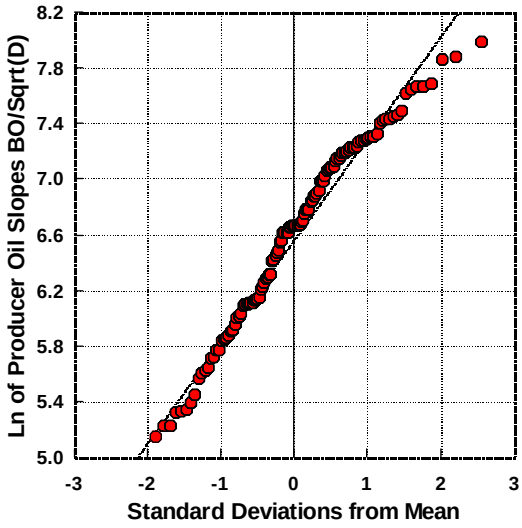

Fig. 16—Order statistics for 121 producers in the Dow-Chanslor Section 1 and 12 prove that their "oil slopes" are lognormally distributed. The intercept of the solid line is the mean and its slope is the standard deviation of the underlying normal population of the oil slope logarithms. Note the excellent fit.

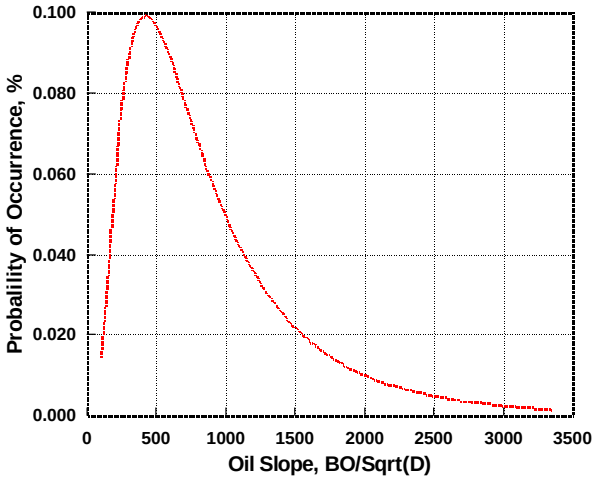

Fig. 17—The lognormal distribution of oil production slopes at Dow-Chanslor. The distribution mode is 420, median is 717 and mean is 937 BO per square root of days on production. The mean plus three standard deviations (99.7% of all wells) is below 3300 BO/Sqrt(D).

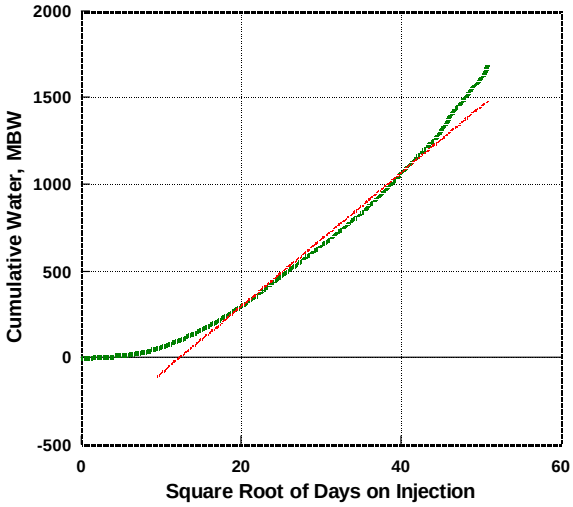

Fig. 18—Cumulative water injection in an average, time-shifted Crutcher-Tufts Section 1 well versus the square root of time. The average water slope for 21 injectors is 34,500 BW per square root of days on injection. Note that the fit is not nearly as good as in Fig. 14 because of the average WHP increases with time.

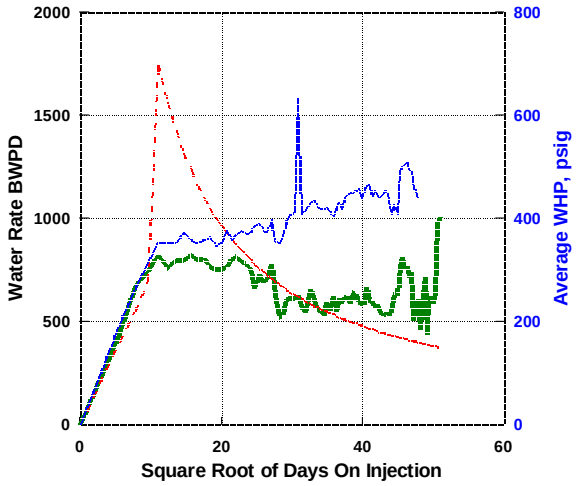

Fig. 19—Water injection rate and pressure (uppermost curve) in an average, time-shifted Crutcher-Tufts Section 1 well versus the square root of time. This is the water injection rate expected from an average well in Section 1, provided that the injection pressure is constant and there is no upper rate limit at early times. Note a 100-day "startup-period."

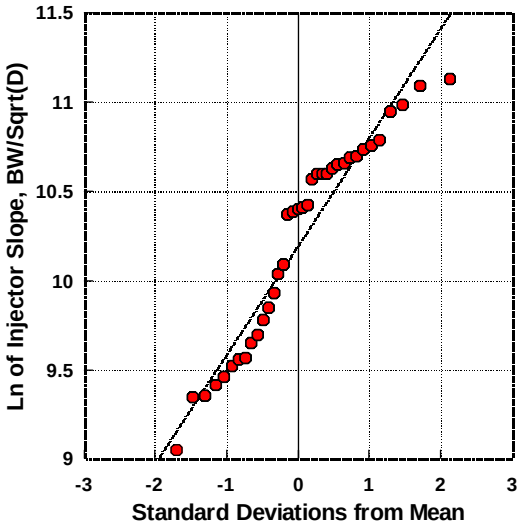

Fig. 20—Order statistics for 37 water injectors in Section 1 and 12 of Dow-Chanslor. The population of "water slopes" is not homogeneous and there seem to be 2-3 underlying sub-populations. Nevertheless, the water slopes are lognormally distributed.

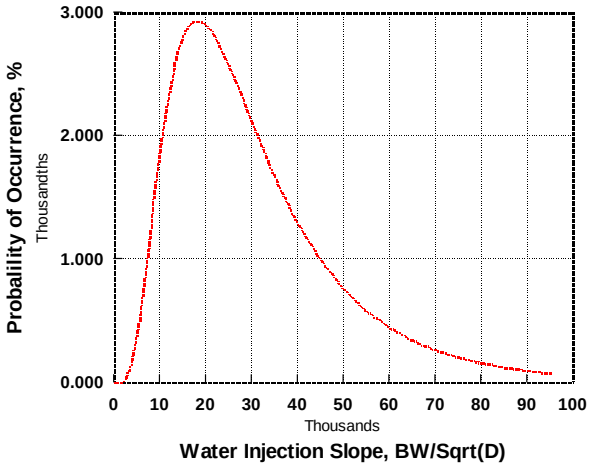

Fig. 21—The lognormal distribution of water injection slopes at Dow-Chanslor. The distribution mode is 18,600, its median is 28,700, and the mean is 32,300 BW per square root of days on injection. The mean plus three standard deviations (99.7% of all wells) is less than 97,000 BW/Sqrt(D).

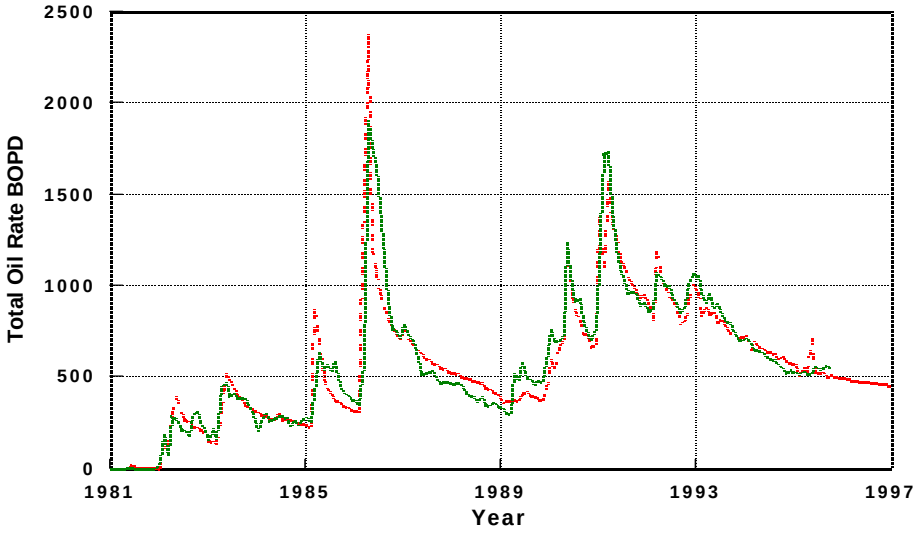

Fig. 22—The actual (solid line) and predicted (broken line) oil production at the Dow-Chanslor Fee, Section 1. Note that the model prediction can be run into the future and additional infill wells can be added, resulting in a very good oil production forecast.

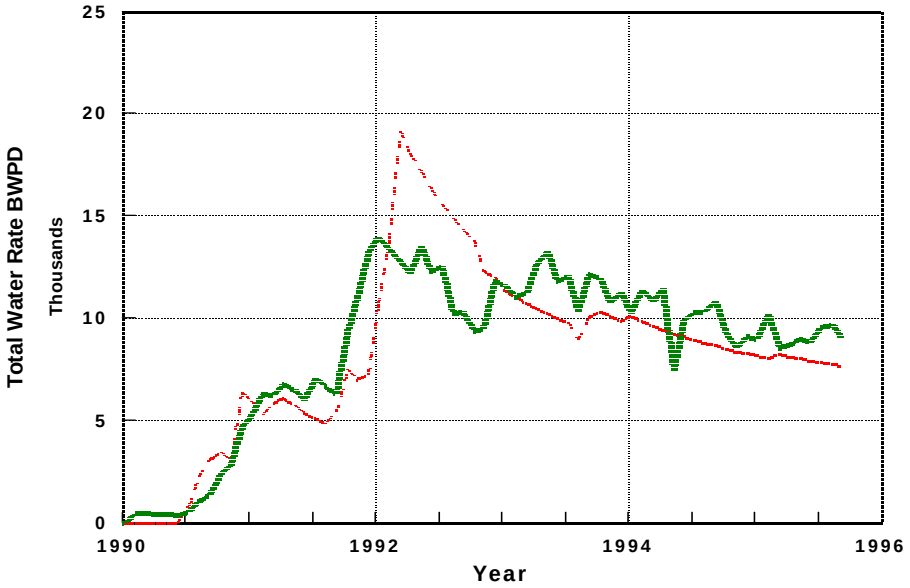

Fig. 23—The actual (solid line) and predicted (broken line) water injection at the Dow-Chanslor Fee, Section 1. Note that the model prediction can be run into the future and additional infill wells can be added, resulting in a reasonably good water injection forecast.